Gold nanoparticles coated with polyvinylpyrrolidone and sea urchin extracellular molecules induce transient immune activation

Gold nanoparticles coated with polyvinylpyrrolidone and sea urchin extracellular molecules induce transient immune activation

Andi Alijagic[a ‡], Francesco Barbero[b ‡], Daniela Gaglio[c,d], Elisabetta Napodano[d], Oldřich Benada[e], Olga Kofroňová[e], Victor F. Puntes[b,f,g], Neus G. Bastús[b], and Annalisa Pinsino[a *]

[a]Consiglio Nazionale delle Ricerche, Istituto per la Ricerca e l'Innovazione Biomedica (IRIB), Palermo, Italy

[b]Catalan Institute of Nanoscience and Nanotechnology (ICN2), CSIC and BIST, Campus UAB, Bellaterra, Barcelona, Spain

[c]Consiglio Nazionale delle Ricerche, Istituto di Bioimmagini e Fisiologia Molecolare (IBFM), Segrate, MI, Italy

[d]SYSBIO.IT, Centre of Systems Biology, University of Milano-Bicocca, Milano, Italy

[e]Institute of Microbiology of the Czech Academy of Sciences, Prague, Czech Republic

[f]Institució Catalana de Recerca i Estudis Avançats (ICREA), Barcelona, Spain

[g]Vall d Hebron, Institut de Recerca (VHIR), Barcelona, Spain

***Corresponding author's email address:** annalisa.pinsino@irib.cnr.it; annalisa.pinsino@cnr.it

‡ **These authors contributed equally.**

Abstract

We report that the immunogenicity of colloidal gold nanoparticles coated with polyvinylpyrrolidone (PVP–AuNPs) in a model organism, the sea urchin *Paracentrotus lividus*, can function as *a proxy* for humans for *in vitro* immunological studies. To profile the immune recognition and interaction from exposure to PVP–AuNP (1 and 10 μg particles mL^{-1}), we applied an extensive nano-scale approach, including particle physicochemical characterisation involving immunology, cellular biology, and metabolomics. The interaction between PVP–AuNPs and soluble proteins of the sea urchin physiological coelomic fluid (blood equivalent) results in the formation of a protein "corona" surrounding the NP from three major proteins that influence the hydrodynamic size and colloidal stability of the particle. At the lower concentration of PVP–AuNPs, the *P. lividus* phagocytes show a broad metabolic plasticity based on the biosynthesis of metabolites mediating inflammation and phagocytosis. At the higher concentration of PVP–AuNPs, phagocytes activate an immunological response involving Toll-like receptor 4 (TLR4) signalling pathway at 24 hours of exposure. These results emphasise that exposure to PVP–AuNP drives inflammatory signalling by the phagocytes and the resolution at both the low and high concentrations of the PVP–AuNPs and provides more details regarding the immunogenicity of these NPs.

Keywords

Sea urchin immune cells; Innate defence response; Nano-recognition; Immune metabolic rewiring; Immunoreactivity

1. INTRODUCTION

Gold nanoparticles (AuNPs) are catching the attention of the scientific community due to the promising progress made in synthesis technologies, in surface functionalization as well as in biomedical, cosmetic and pharmaceutical applications[1]. A wide variety of specific properties (e.g., small size and associated high surface to volume ratio, particle stability, low cost to produce, electronic, magnetic and optical properties) makes AuNPs an ideal material for bioimaging, gene diagnostics, cancer therapy, and drug delivery[2]. Accordingly, safety assessment becomes an important issue for the beneficial usage of this new nanomaterial. However, increasing nanobiotechnological applications result in the increased exposure of all living organisms and the environment to NPs. This exposure, which is assumed to increase in the future, justifies the need to identify, measure and manage the presumed risk. Chemical transformations of NPs in the environment are poorly understood at present, largely due to the complexity arising from concurrent transformations (e.g., oxidation, sulfidation, reduction reactions, surface adsorption of macromolecular and ions) by the action of sunlight and microorganisms, as well as oxidants[3]. There are a few analytical methods to determine the level of occurrence and the fate on AuNPs in water, soil, air and biological matrices. In a realistic scenario, colloidal AuNPs may be trapped by the sediment becoming unavailable for the majority of the organisms. However, filter feeders and other species associated with the sediment may be the exceptions because they take up particles including AuNPs that incorporate them into the food chain and undergoes biomagnification[4]. At present, there are significant gaps in our knowledge of how gold particles impact human health because of their chemical and physical properties but also because of complex interactions that may occur at various biological levels including genes, transcripts, metabolites, proteins, enzymes, organelles, cells, tissues, organs, organ systems, and whole organisms. Nano-structured materials display a privileged interplay with the effector cells of the immune system, especially phagocytic cells, which, once activated, recognize, interact, and eliminate foreign particles[5].

The wide use of AuNPs strengthens concerns regarding their safety and compatibility with the innate immune system, which is the primary defensive barrier that functions continuously, both in healthy and diseased organisms. Although many aspects of the modulation of immune responses induced by AuNPs have been investigated, results remain controversial[6]. AuNPs interact with the immune system and induce downstream immune and inflammatory signalling that may both support and suppress inflammation[6]. For example, macrophages engulf 3 nm-AuNPs efficiently through the process of pinocytosis, without eliciting a pro-inflammatory cytokine release (e.g., tumour necrosis factor-α, interleukin 1)[7]. In contrast, a different immunological scenario that is marked by a pro-inflammatory reaction (e.g., up- or down-regulation of IL-1, IL-6, TNF-α) is evident when cells interact with AuNPs of different size and/or functionalized surface[8-10]. In assessing the

immunogenicity of the AuNPs, it is important to give consideration not only to the particle size but also to other biologically relevant properties (e.g., stability, dispersibility, reactivity) on which depends their ability to recognize or to be recognized by cells. Because AuNPs tend to aggregate/agglomerate in a biological medium[11], the surface functionalization of the AuNPs may be considered necessary to enhance both their stabilization and dispersibility in that medium.

Although nude particles can be toxic, coated particles (e.g., PVP, humic acid, serum) can be harmless because the acquired chemical functions of the coat modify the properties of the NPs, which influence bioavailability and biocompatibility. Biocompatibility is mandatory when the NPs are used for applications that they be inert as in some medical, industrial and environmental applications. On the contrary, targeting the immune system with NPs can be used to stimulate or inhibit the medical applications that can be anti-inflammatory, anti-cancer, anti-viral therapies[12-13]. This emphasizes the basis for the great level of interest concerning the immunogenicity or immunocompatibility of AuNPs.

The 3R principle of reducing, refining, and replacing animal experimentation has led to new methodologies for *in vivo* and *in vitro/ex vivo* investigations, with increasing use of invertebrate animal models, including the chance of "substituting" mammalian models with invertebrates[14]. Based on this aim, the Mediterranean sea urchin, *Paracentrotus lividus*, a marine invertebrate, has become a swift and efficient popular model that is a *proxy for humans* for basic and translational nano-immunological studies *in vivo*[15-16] and, more recently, *in vitro/ex vivo*[17-18]. The genome sequence of a different sea species emphasised some strong similarities between sea urchin and human immunity, and also identified clues of the basis of alternative adaptive and anticipatory immune functions that are shared with humans[19].

To profile the sea urchin immune cell behaviour resulting from exposure to PVP–AuNPs at varying concentrations (1 and 10 μg mL^{-1}), here we focus on the: i) characterisation of PVP–AuNPs in the sea urchin coelomic fluid (CF), in which immune cells secrete functional biomolecules; ii) behaviour of PVP–AuNPs (stability, dissolution, aggregation and particle transformation) in the CF with a special focus on the main constituents shaping sea urchin PVP–AuNP protein corona; iii) sea urchin phagocytic cell topography and related PVP-AuNP surface distribution; iv) defensive innate/inflammatory signalling leading the immune-PVP–AuNP recognition and interaction *in vitro*. We demonstrate that protein-particle interaction triggers an extended network of immune-related signalling, drawing a transient immune activation both at the low and the high concentrations of the particles.

2. MATERIALS AND METHODS

2.1 Polyvinylpyrrolidone-functionalized gold nanoparticle synthesis and characterisation.

Chemical precursors. Tetrachloroauric (III) acid trihydrate (99.9% purity), sodium citrate tribasic dihydrate (≥99% purity), polyvinylpyrrolidone (PVP) (55 kDa) were purchased from Sigma-Aldrich.

AuNP preparation. Citrate-stabilized AuNPs were synthesised according to the previously developed seeded-growth methods[20]. Briefly, sodium citrate (Na_3Ct; 2.2 mM) in milliQ (mQ) water was boiled in a three necks flask under reflux, followed by the addition of chloroauric acid ($HAuCl_4$; 25 mM). The citrate-stabilised AuNPs solution-phase synthesis was completed within a few minutes and produced ~10 nm NP seeds. Following seeding, the desired size of the Na_3Ct-coated AuNPs was obtained by sequential growth steps.

AuNP surface coating process by PVP and sample purification. PVP (0.2 mM) in mQ water plus Na_3Ct-coated AuNPs (100 μg mL^{-1}) was stirred overnight. PVP-AuNPs were purified from the excess of PVP by centrifugation (15 000 x *g*), the supernatant was aspirated, and particles were resuspended in mQ water. Samples were washed twice in mQ water, and the final PVP-AuNP concentration was 2 μM PVP coating on 100 μg mL^{-1} AuNPs.

PVP-AuNP characterisation. Particle microstructural characterisation was carried out using a scanning electron microscope (SEM; FEI Magellan 400 XHR; eXtreme High Resolution) operated at 20 kV. PVP-AuNPs were prepared by applying 4 μL onto a carbon-coated copper transmission electron microscopy (TEM) grid and dried at room temperature (RT). PVP-AuNPs (922 particles) from different regions of the grid were analysed.

UV-Vis Spectroscopy analyses. PVP-AuNPs (1 and 10 μg mL^{-1}) were analysed for their behaviour in a high salt solution (Coelomocyte Culture Medium; CCM[21]) and biological medium (sea urchin cell-free CF in CCM; 1:1 diluted) [22]. Specifically, 1 mL of each sample was placed in a plastic cuvette, and the spectral analysis was performed in an Agilent Cary 60 spectrophotometer (300−900 nm range, at RT). The concentration of particles in mQ water was used as reference baseline value to normalize that particle concentration of each sample.

Size and Zeta Potential Measurements. The hydrodynamic diameter of the PVP-AuNPs before and after incubation in CCM was determined by dynamic light scattering (DLS), and laser doppler velocimetry respectively, using a Malvern Zetasizer Nano ZS instrument equipped with a light source wavelength of 638.2 nm and a fixed scattering angle of 173°. Diameters of the NPs were reported as intensity distribution calculated by non-negative least squares (NNLS) analysis; and as Z-average and polydispersity index (PDI) calculated by cumulant analysis. The software was arranged with the parameters of the refractive index and absorption coefficient of gold, and solvent viscosity of water at 25°C.

2.2 Animal collection and maintenance, immune cell cultures and exposures.

Adult sea urchins (*Paracentrotus lividus*) were collected along the coasts of Sicily (Italy) that are not human-impacted. Animals were acclimated for 1 week and kept under strictly controlled conditions in tanks provided with flow-through oxygenated artificial seawater (Aqua Ocean Reef Plus Marine Salt, Aquarium Line, Italy; salinity (38–39‰) and density (1.028–1.030 g/cm^3)). Artificial seawater ensures the absence of pollutants or organic matters putatively present in the natural seawater, which could affect the sea urchin immune response. CF containing immune cells was harvested from each donor in a medium containing ethylene glycol tetra-acetic acid (EGTA; 1 mM) in CCM. Cells in the CF were withdrawn with a syringe preloaded with CCM and diluted 1:1. After collection, half of the diluted CF was placed in culture and exposed to the NPs. The rest of the CF was centrifuged, the cells were discarded, and the cell-free CF was exposed to NPs based on standard procedures established for these experiments (see nanoparticles conditioning and protein corona profiling section). Primary immune cell cultures were established following the procedures recently described in Pinsino and Alijagic[22]. Briefly, harvested immune cells from eight healthy donors were exposed to increasing concentrations of PVP-AuNPs (0, 0.1, 1.0, and 10 μg mL^{-1}), and maintained in a custom-made cell culture incubator at 16±2°C, for 24 hours (h). Cells were collected by a soft scraper, centrifuged at 9000 x g for 10 min at 4°C and stored at -80°C. Experimental conditions (*e.g.,* particle concentrations, exposure time) were set taking into account: i) the behaviour of AuNPs in salt water media[23-24]; ii) the detection limits of DLS for polydispersed colloids[25]; iii) the high ionic strength of CCM[22].

2.3 Real-time viability assay.

Cell viability of immune cells obtained from five sea urchins was assessed in a real-time measurement using the non-lytic and bioluminescent RealTime-Glo MT Cell Viability Assay (Promega, USA) as previously reported[22]. Luminescence was calculated using GloMax Discover high-performance Microplate Reader (Promega, USA). PVP-AuNPs were incubated alone with reagents to identify any possible interference by the particles with the assay.

2.4 Microscopy.

Scanning electron microscopy coupled with energy-dispersive X-ray spectroscopy. Immune cells exposed to PVP-AuNPs (1 and 10 μg mL^{-1}, 24-h exposure) that adhered to glass coverslips (Menzel Gläser, Germany) were fixed and prepared for SEM as reported previously[17]. Cell morphology was observed with a FEI Nova NanoSEM scanning electron microscope (FEI, Brno, Czech Republic) and the EDS microanalysis was performed by Ametek® EDAX Octane Plus SDD detector and TEAM™ EDS Analysis Systems (Ametek, Inc.). Predictive theoretical model spectra were made using the NIST DTSA-II Kelvin software package[26-27].

Immunofluorescence microscopy. Immune cells were distributed in wells of a 25-well plate (Thermo Fisher Scientific) and incubated with 10 μg mL^{-1} AuNPs for 24 h. Cells were fixed with ice-cold methanol for 20 min and washed three times in CCM. Non-specific binding sites were blocked with blocking buffer (3% bovine serum albumin (BSA), 5% inactivated normal goat serum (NGS), 0.02% Triton X-100 in TBST) for 2 h, at RT. After blocking, cells were incubated overnight at 16±2°C with anti-TLR4 (H-80) (Santa Cruz Biotechnology, sc-10741) and anti-α-tubulin (SIGMA, T5168) both diluted 1:50 in blocking buffer. Cells were washed three times in TBST and incubated for 1 h at 16±2°C with the secondary antibodies; i) goat anti-mouse-IgG (IRDye® 800CW, LI-COR) and ii) goat anti-rabbit- F(ab')2 fragment (Alexa Fluor® 594, Life Technologies) both diluted 1:200 in blocking buffer. Cells were incubated with Hoechst dye (Hoechst 33342; 3 μM) for 7 min to visualize nuclear DNA. Photomicrographs of immune cells were acquired with the Leica fluorescence microscope using the 40x objective.

2.5 SDS-PAGE and immunoblotting.

Cellular pellets were homogenised in a standard lysis buffer in preparation for SDS-PAGE complemented with phosphatase and protease inhibitor cocktails[28]. Protein content of samples were quantified by the BioRad assay kit (Hercules, CA, USA) followed by precipitation overnight at −20°C in equal volume of acetone. Proteins pellet were resuspended immediately in SDS buffer containing β-mercaptoethanol, denaturized at 100°C for 5 min plus cooling for 5 min, separated on polyacrylamide gels (4–20% Mini-PROTEAN TGX precast BioRad, USA), and transferred to nitrocellulose membranes (Amersham, UK), according to the manufacturer's instructions. Following blocking, membranes were incubated with one of the following primary antibodies: anti-TLR4 (H-80) (Santa Cruz Biotechnology, sc-10741; diluted 1:250 in blocking buffer; anti-HSP70 (SIGMA, Cat N. H-5147, 1:1000); anti-phospho-p38 MAP Kinase (Tr180/Tyr182) (Cell Signaling, 9211, 1:250); Phospho-p42/44 MAP Kinase (ERK1/2) (Cell Signaling, 9101, 1:300); IL-6 (H-183) (Santa Cruz Biotechnology, sc-7920, 1:100); anti-MnSOD (Enzo Life Sciences, ADI-SOD-111, 1:200); anti-NF-κB (H-286) (Santa Cruz Biotechnology, sc-715, 1:200); anti-β-actin (SIGMA, A5441, 1:500); anti-*Pl*-toposome (BEVIB12b8[29], 1:200); anti-*Pl*-nectin[30], 1:200); anti-*Pl*-galectin-8[31], 1:800). Following washing, membranes were incubated with fluorescein-labelled secondary antibodies (LI-COR Biosciences) and protein bands were visualised and captured by the Odyssey Infrared Imaging System (LI-COR Biosciences).

2.6 Nanoparticles conditioning and protein corona profiling.

PVP-AuNP (1 and 10 μg mL^{-1}) were added to 1 ml of cell-free CF diluted in equal volume of CCM (cell-free CF in CCM) in TreffLab 1.5 mL microcentrifuge tubes and incubated with agitation (shaking platform; bioSan, Latvia) for 24 h at 16±2°C in the dark. After incubation, the PVP-AuNPs

with newly-formed protein complexes were recovered by centrifugation at 21130 x g for 20 min at 4°C, followed by three energetic rinses in artificial seawater as already described[17]. PVP-AuNP-protein-complex pellets were resuspended in Laemmli buffer containing β-mercaptoethanol (Bio-Rad, USA), boiled for 5 min, and the PVP-AuNPs were pelleted at 21130 x *g* for 20 min at 4°C. Eluted proteins were separated on polyacrylamide gels (4–20% Mini-PROTEAN TGX precast Bio-Rad, USA) that were stained with Coomassie Brilliant Blue R250 to identify the protein bands. Protein binding to the PVP-AuNPs were performed four times with cell-free CF from different sea urchins to ensure reproducibility. Gel scans were processed by the ImageJ software (NIH, USA).

2.7 Metabolomic typing by untargeted liquid chromatography and mass spectrometry.

Liquid chromatography-mass spectroscopy (LC-MS analysis) was performed according to previously established protocols[18]. Cells exposed to PVP-AuNPs (1 μg mL^{-1}, 24-h exposure) were gently recovered from the culture plate, centrifuged at 4500 x g for 5 min at 4°C, and pellets were resuspended in 0.5 mL ice-cold 70% acetonitrile (Sigma-Aldrich). The supernatant fraction containing both polar and non-polar metabolites was retrieved in glass vials followed by solvent evaporation and drying at 30°C. Samples were resuspended in 150 μL of ultrapure water and injected in the UHPLC–MS system to be analysed by reversed-phase chromatography[18]. Mass spectra were recorded in a mass range of m/z 60 to 1050 m/z (centroid mode). A mass correction was performed through a second nebuliser by a reference solution (m/z 112.9855 and 1033.9881) dissolved in the mobile phase of 70% 2-propanol-acetonitrile-water. Analysis and isotopic natural abundance data correction were performed by MassHunter ProFinder and Mass Profile Professional software (Agilent).

2.8 Statistical Analysis.

Statistical analyses were performed by GraphPad Prism Software 6.01 (USA). Statistical differences among selected groups were estimated by one-way or two-way ANOVA (followed by the multiple comparison tests). A *p*-value of less than 0.05 was deemed statistically significant. Data were reported as mean ± standard deviation (SD) or mean ± standard error (SE).

3. Results and discussion

3.1 Extracellular molecules in the cell-free CF affect stability and aggregation kinetics in a high salt medium.

Physicochemical properties of NPs determine their safety, stability, efficacy, as well as their *in vitro* and *in vivo* behaviour. The leading mechanisms involved in NP transformation may depend on the size and the concentration of the particles, the route of exposure to biological molecules, the

NP physicochemical features (*e.g.*, surface chemistry, size, shape, geometry) and the nature of the environment in which the particles are found[32]. Metallic NPs such as AuNPs tend to form colloidal aggregates and the stability of these particles is based on a balance between the electrostatic repulsion and the universal attractive van der Waals force described by the DLVO theory. Salt concentrations of the fluids tend to reduce electrostatic repulsions between head-to-head NPs and favours homo-aggregation, whereas the organic matters suspended in the fluids may aid in hetero-aggregation[33]. Aggregation influences the fate of the NPs in the environment, particularly in aqueous environments, which depends on ionic strength and composition, organic matter composition and pH. These chemical and biochemical attributes may affect the particle surface charge stability, and in turn, particle bioavailability and dispersion. Results from environmental monitoring of AuNPs *in situ* are not available, and therefore *in silico* modelling of the particle behaviour is currently the only means for estimating exposure to organisms[34].

The appropriateness of NPs for a specific application in medicine, cosmetic and pharmaceutical applications, depends on their average diameter, PDI and size, among other parameters. Measurements of PVP- AuNPs showed a core diameter of 25.0 ± 3 nm (Figure 1A, upper panel). However, the physicochemical characterisation of PVP-AuNPs (10 µg mL^{-1}) in CCM had a hydrodynamic diameter of 63 nm with a polydispersity index of 0.122 (Figure 1A lower panel). The zeta potential value in water was -15.3 ± 0.6 mV (conductivity 0.006 mS/cm), whereas the zeta potential value in CCM was near neutral. This was because electrostatic charges were efficiently screened when the ionic concentration of the solution was very high[35] as well as for the non-ionic nature of the polymer[36]. The UV-vis spectrum of PVP-AuNPs (10 µg mL^{-1}) dispersed in both CCM (Figure 1B, red and blue lines) and mQ water (Figure 1B, green line) presented a typical profile of monodisperse particles with a maximum size dispersion of 524 nm. UV-vis values did not show significant changes in dynamic absorption at 0 h. Notably, at 24 h of exposure in CCM, a weak decrease (<10%) in absorbance was noted but there were no changes in the UV-vis profile and DLS (Figure 1B, compare red and blue line). This change simply suggested a reduction in the PVP-AuNP concentration in the solution. It may be that even if PVP-AuNPs remain well dispersed in high salt solutions, the increment of the polarity of the solvent may decrease their dispersibility. This would lead to a partial adsorption of the PVP-AuNPs to some types of plastics or to glass surfaces, which may modify their dissolution kinetic and related dispersibility depending on the material employed. However, a partial loss of PVP coating AuNP cannot be excluded[37]. Overall, these data indicate good monodispersity and stability of the particles also after suspension in CCM with high salt concentration, including the chelating agent, EGTA that blocks cell aggregation[21], NaCl, $MgCl_2$ and HEPES. Remarkably, the immune cells are collected from *P. lividus* in CCM because this medium maintains the sea urchin cell density and salinity very close that of the sea urchin CF, and it preserves the morphological features of cells and blocks calcium-dependent cell clotting[22].

The UV-vis spectrum of the PVP-AuNPs after 24 h of exposure to cell-free CF *plus* CCM resulted in significant differences in both the shape and absorbance of the NPs, indicating that PVP-AuNPs interacted with sea urchin extracellular biomacromolecules and led to the formation of hetero-aggregates of particles of both concentrations (Figure 1C and D, blue lines). The decreased absorbance values were related to both increased aggregation and decreased measurable particle concentration under static conditions, as confirmed by the presence of noticeable precipitates. After shaking to disperse the precipitates, samples showed similar spectra but increased absorbance and baselines to that of static conditions (Figure 1C and D, dashed blue lines). This is due to the light scattering effects that are common for larger NP aggregates. Our findings indicate that samples underwent fast flocculation mediated by organic matter that created larger hetero-aggregates (biomolecule-particle complexes) which are easier to dissociate than homo-aggregates (particle-particle aggregation). Notably, at 1 μg mL^{-1}, the AuNPs showed slower aggregation, as expected. The UV-vis spectrum of the PVP-AuNPs (1 and 10 μg mL^{-1}) dispersed in cell-free CF *plus* CCM at 0 h showed similar results to those obtained from CCM alone when evaluated at the same particle concentration (compare Figure 1C and Figure 1B, red lines), as expected.

Biomacromolecules are able to change NPs properties, including their stability and related interactions among particles[38]. The balance between homo- and hetero- aggregation scenarios is driven by the relative collision frequencies of NPs together and with organic components, respectively[39]. Polymer coatings, including PVP, are stable under unperturbed conditions but other ligands can well replace them[40]. Critically, our findings support the notion that CF biomacromolecules may replace the PVP onto the AuNP surface, but this replacement is not able to confer a satisfactory particle steric stabilisation. PVP-organic macromolecule exchanges onto the AuNP surface are probably related to the stronger protein chemical moieties interaction than that of the cyclic amide groups of the PVP[41] (see below). We found that the interaction between sea urchin extracellular organic matter and PVP-coated AuNPs formed a dynamic biomolecule coating causing a lost in particle steric stabilisation, which induced a colour change of the biological medium from red to purple (Figure 1E), indicative of particle aggregation[42]. AuNP aggregation correlated with the extracellular protein adsorption onto the particle surface is a well-noted process in mammalian immune cell culture[43].

Stabilising agents such as PVP play an important role in the corona formation as they minimise the protein adsorption compared to that of an uncoated particle surface, in which an increase in the conformational entropy and a decrease in the Gibbs free energy change, promote a strong particle/protein interaction[44]. The capability to modulate the functional composition of the protein corona is critical for the design of ideal and safe NPs because permit to modulate the bio-accessibility and the nanotoxicity of the particles for guiding their design, synthesis, and effective applications in

nanomedicine. In agreement, control over the protein corona of NPs by using PVP allows them to function better as drug delivery vehicles because decrease their cytotoxicity[45].

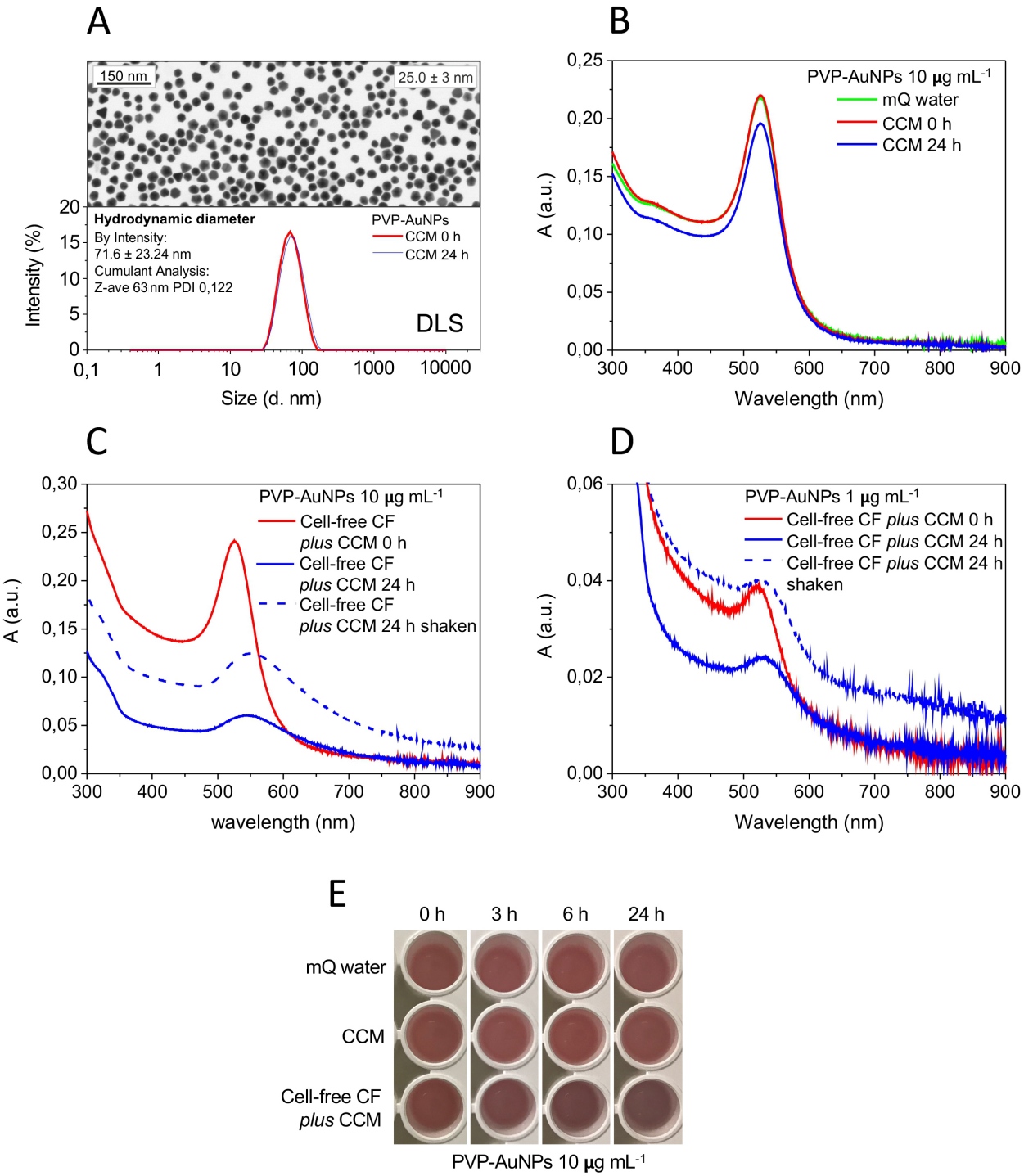

Figure 1. Physicochemical characterisation of PVP-coated AuNPs dispersed in CCM and cell-free CF *plus* CCM. (A) SEM image of PVP-AuNPs in CCM (upper panel); DLS size measurement of PVP-AuNPs (10 µg mL^{-1}) dispersed in CCM at 0 and 24 h time period of exposure (lower panel, red and blue line). (B) UV-vis spectra of PVP-AuNPs (10 µg mL^{-1}) dispersed in mQ water, 0 and 24 h time period (green line) and in CCM at 0 h (red line), and in CCM at 24 h of exposure (blue line). (C) PVP-AuNPs dispersed in **cell-free** CF *plus* CCM at 10 µg mL^{-1} and 0 and 24 h of exposure (red line, and blue line respectively). (D) PVP-AuNPs dispersed in **cell-free** CF *plus* CCM at 1 µg mL^{-1} and 0 and 24 h of exposure (red line, and blue line respectively). (E) Macroscopic changes of PVP--coated AuNPs (10 µg mL^{-1}) dispersed in mQ water, CCM, and cell-free CF *plus* CCM, from 0 to 24 h of exposure. The biological medium (cell-free CF *plus*

CCM) changes colour from red to purple over the 1 day of monitoring. In C and D, dashed blue lines indicate spectra of shaking sample at 24 h of exposure. Physicochemical characterisation of PVP-coated AuNPs dispersed in the mQ water has been used as the reference point.

3.2 Sea urchin immune system interactions with PVP-AuNPs *in vitro*.

The immune cells (phagocytes, amoebocytes and vibratile cells) in the sea urchin, *P. lividus*, are morphologically distinct with different functions and act as the defence system for protection against exogenous and endogenous menaces to the host[46]. The phagocytes can be found in both filopodial and lamellipodial morphology, are highly adherent, and are the most abundant (up to 80%) cell type present in the sea urchin CF. They are associated with phagocytosis and encapsulation of foreign invaders, allograft rejection, cytolytic/cytotoxic and inflammatory responses, antimicrobial peptide secretion, etc[47]. To initiate our understanding the immune nanoscale interaction with PVP-AuNPs, we focused on sea urchin immune cell topography and the distribution of PVP-AuNPs (1 and 10 μg mL^{-1}) on and within cells after 24 h of exposure *in vitro*. Observations by SEM coupled with EDS showed that cells were spread and adherent to the culture plate (Figure 2A, 2D) as well as organised in bundles and fibres at the lower concentration of PVP-AuNPs (Figure 2A, blue arrowhead). The composition of the electron-dense gold particles was confirmed by EDS (see Figure 2S). Particle aggregates/agglomerates that were displayed on cell surfaces ranged in size from 0.195 to 1.6 μm in diameter (Figure 2A-F, yellow boxes). This association suggested a tight adhesion between the PVP-AuNPs and the cell surfaces (Figure 2B, 2E; Figure 2C, 2F back-scattered electron images) that may have occurred by the interaction between cell surface receptors and sea urchin extracellular protein ligands on the PVP-coated AuNP biocorona. Notably, back-scattered electron approach permitted imaging that could discriminate both organic (dull shine) and inorganic (intense brightness) materials inside of the cells (see Figure 2C, 2F), in agreement with Goldstein et al[48]. Particle aggregates/agglomerates were located at the outer and the inner surface of the plasma membrane (Figure 2B and 2E, yellow boxes; and Figure 1S). The SEM images suggests that sea urchin phagocytes are able to take up PVP-AuNP aggregates/agglomerates. The composition of the electron-dense gold particles was confirmed by EDS (see Figure 2S). The number of PVP-AuNP aggregates/agglomerates that immune cells may takes up and accumulate, may be related to particle concentration (see aggregates in Figure 2B, 2E). To the contrary, aggregate/agglomerate size may to be independent of the concentration used (see Figure 2C, 2F). The general healthy state of sea urchin immune cells in culture and exposed to PVP-coated AuNPs was monitored over three days of the experiment by the RealTime-Glo MT Cell Viability Assay for cells exposed at increasing concentrations of the NPs (0.1, 1, 10, μg mL^{-1}) (see Figure 3, three measurement points are shown). The viability of the cells incubated with PVP-AuNPs (0.1, 1 μg mL^{-1}) over three days was not different from the control cells that were cultured in the absence of NPs.

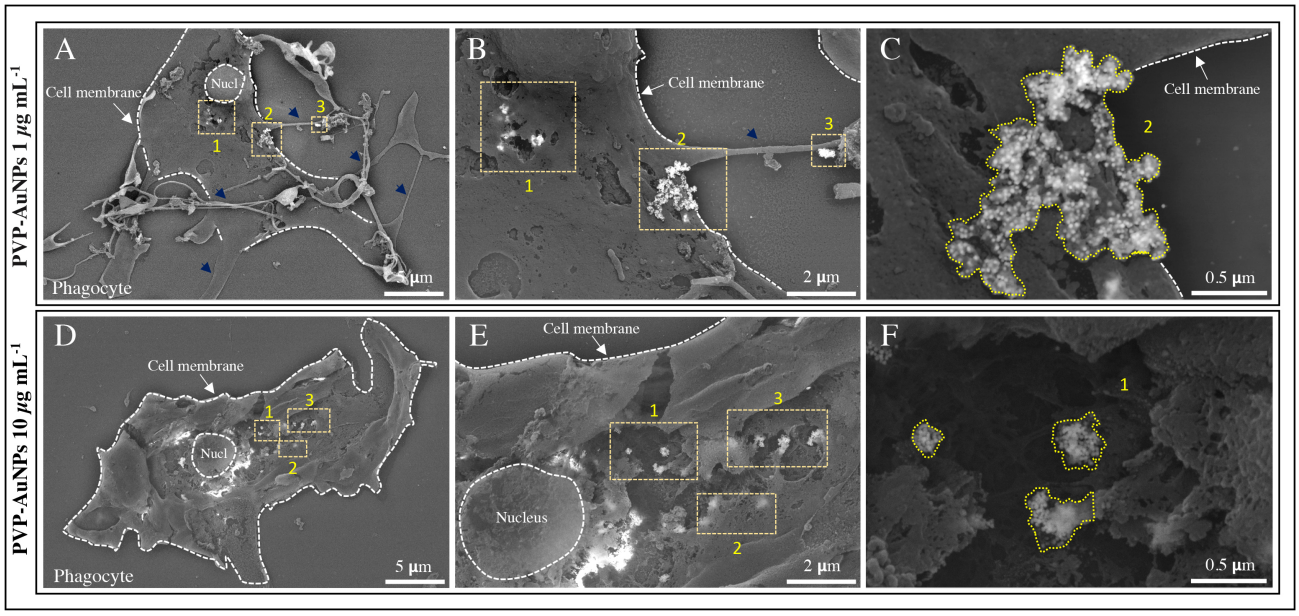

Figure 2. Scanning electron microscopy shows the interaction between PVP-AuNPs and sea urchin immune cells *in vitro*. (A-C) Phagocytes exposed to 1 μg mL^{-1} PVP-AuNPs for 24 h. (D-F) Phagocytes exposed to 10 μg mL^{-1} PVP-AuNPs for 24 h. Back-scattered electron image (A, D) low-magnification (B-C, E-F) high-magnification. Yellow boxes highlight aggregates/agglomerates at the outer and the inner surface of the plasma membrane.

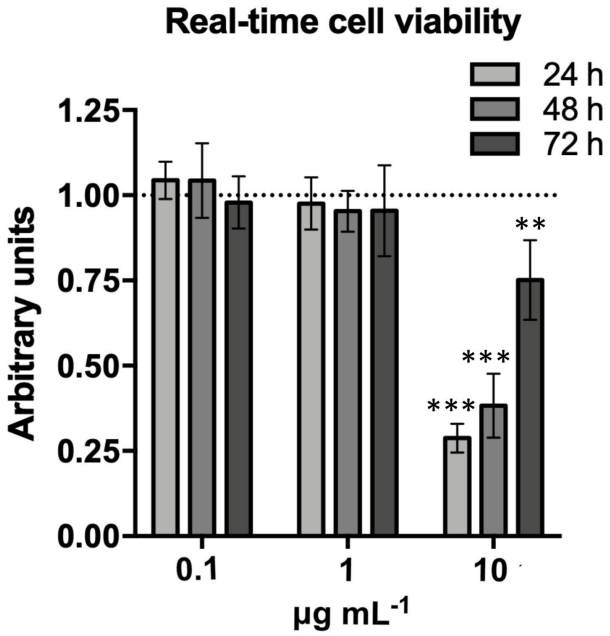

Figure 3. Real-time viability assay reveals the impact of increasing concentrations of PVP-AuNP on sea urchin immune cells in culture. Cell viability during three days of continuous monitoring shows three measurement points (24, 48, 72 h) for three difference concentrations of PVP-AuNPs (0.1, 1, 10 μg mL^{-1}). Only the highest dose of PVP-AuNPs (10 μg mL^{-1}) results in a decrease in cell viability. Levels are expressed in arbitrary units as fold increase or decrease compared to controls that were set to 1 (dotted line). Data are reported as the mean ± SD; asterisks (*) indicate significant differences among groups (**$p < 0.01$; ***$p < 0.001$).

On the contrary, the viability was significantly decreased for cells incubated with the highest NP concentration (10 μg mL^{-1}) compared to unexposed cells, which was in line with the reduced ability of the cells to form dendritic protrusions as bundles and fibres across the surface of the plate. In agreement with previous reports, AuNP exposure causes disruption in the cytoskeletal filament

content of human dermal fibroblast[49]. However, the level of viability in the cells exposed to PVP-AuNPs (10 μg mL^{-1}) for 1 day was lower than that for three days, perhaps because these cells were under recovery. We speculate that the sea urchin immune cells may have responded to a sub-toxic exposure to PVP-AuNPs that activated a tolerogenic immunological response, possibly promoted by excretion of the particle content. In vertebrates, a stimulus may induce a re-programming of the immune system, resulting either in reduced reactivity (tolerance) or increased response (potentiation) to a challenge[50].

To elucidate whether extracellular proteins mediate the interactions between sea urchin phagocytes and PVP-AuNPs, particles (1 and 10 μg mL^{-1} final concentration) were incubated with cell-free CF collected from donor sea urchins and diluted in the CCM (1:1) for 24 h. Profiles of the *P. lividus* extracellular proteins adsorbed onto and extracted from the PVP-AuNP surface showed that PVP-AuNPs-protein complexes were composed of three major proteins of about 170, 100, and 40 kDa (Figure 4, black asterisks). The type of proteins adsorbed to the particles likely plays a key role in cellular recognition, uptake, and removal mechanisms of AuNPs[51]. Engineered metal nanoparticles are able to acquire a biological identity in contact with the sea urchin CF based on both selective and non-selective affinity[17]. Here, PVP-AuNPs presented the strongest selective affinity for the protein of about 40 kDa while, for example, TiO_2NPs have the greatest affinity for the protein of about 100[17], confirming that each type of NPs acquires a selective biological identity which will define the recognition of the NPs by the immune cells and their subsequent interactions. The effectiveness of nanomaterials for biomedical purposes strongly depends on both the successful NP-uptake by cells and their tolerogenic immunological response[52].

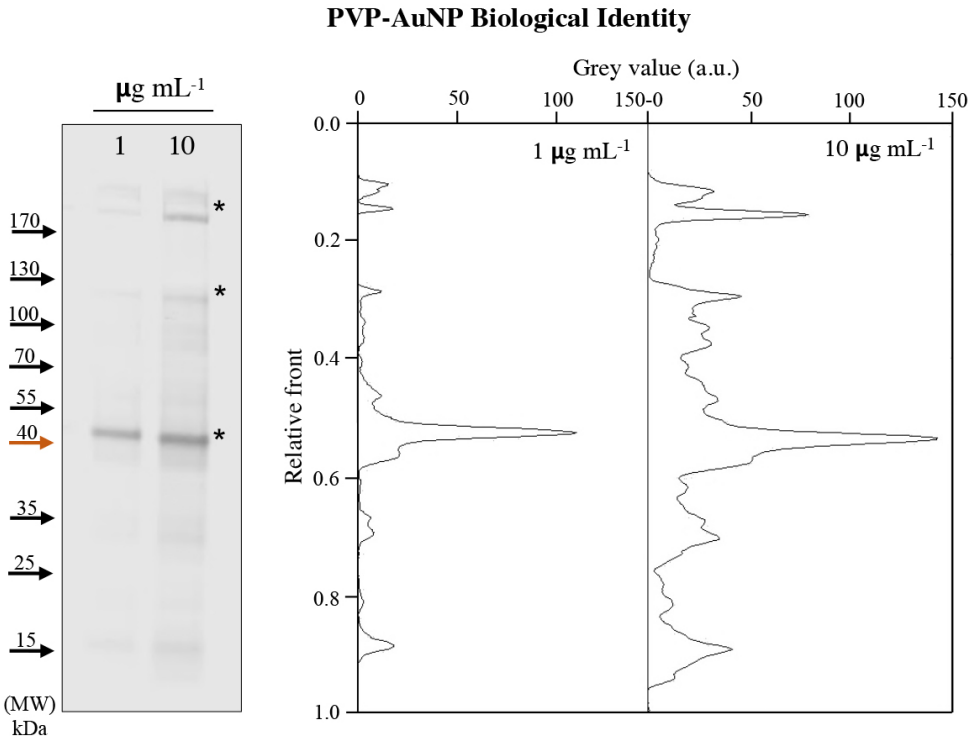

Figure 4. PVP-AuNP acquire a biological identity in contact with the sea urchin CF based on three major proteins. SDS-PAGE profiles the extracted protein corona acquired from cell-free CF *plus* CCM onto PVP-AuNPs (1 and 10 µg mL^{-1}) after 24 h of incubation (left panel). Intensity analysis of the associated spectra profiles performed by the ImageJ software (NIH, USA) (middle and right panels).

3.3 Sea urchin phagocytes undergo metabolic rewiring to control inflammatory responses upon exposure to PVP-coated AuNP *in vitro.*

Mammalian phagocytes function to remove foreign invaders, and apoptotic inflammatory cells, and to remodel the extracellular matrix. These innate immune cells also secrete cytokines, chemokines, and growth factors leading their polarisation from a pro-inflammatory and the activation of an immune response to anti-inflammatory and the resolution of a response[53]. The cellular metabolism represents the key to this functional plasticity by providing energy and chemical constituents (metabolites) that are necessary to coordinate immune cell proliferation, quiescence, differentiation, and the production of secretory molecules for managing intracellular and extracellular signals. To obtain integrated information on that state of phagocyte immune-metabolism and associated tolerance, we employed LC-MS to characterise the metabolic profile of sea urchin immune cells exposed to PVP-AuNPs (1 µg mL^{-1}) for 24 h. We used the low concentration of NPs because no harmful effects on the biological activities of the exposed cells were identified (see Figure 2 and Figure 3). A hierarchical clustering heatmap was used to highlight the level of changes of 22 metabolites comparing un-exposed sea urchin immune cells (group 1) to immune cells exposed to PVP-AuNPs (group 2). Results included analyses of amino acids (L-threo-3-methylaspartate, glutamic acid, taurine, phenylalanine, glycine, glutamine), amino acid intermediates (O-acetylserine),

nucleotides (inosinic acid also known as inosine monophosphate, nicotinamide adenine dinucleotide [NAD], guanosine monophosphate [GMP], uridine monophosphate [UMP], cytidine), organic acids (aconitic acid, D-threo-isocitric acid, citric acid, N-acetylneuraminic acid, arachidonic acid, juniperonic acid), enzymes (dehydroascorbate, 2,5-didehydro-D-gluconate), and sulfate metabolites (sulfate) (Figure 5). Metabolites from phagocytes responding to PVP- AuNPs were predominantly involved in mediating inflammatory response and phagocytosis. Specifically, inosinic acid and NAD and GMP were found significantly increased in exposed cells compared to the controls; while sialic acid and sulfate metabolites were significantly decreased. Inosinic acid exerts a broad range of anti-inflammatory effects (e.g., down regulation of TNF-α, IL-1, IL-6 and MIP-2) in animal models with acute respiratory distress syndrome[54]. Induction of NAD synthesis regulates both macrophage polarisation and phagocytosis, and refurbishes oxidative phosphorylation and cellular homeostasis[55]. Phagocytosis efficiency is reduced when NAD salvage synthesis is inhibited[56]. Consequently, the significantly increased NAD levels observed in phagocytes responding to PVP-AuNPs (1 μg mL^{-1}) may be a signature of increased phagocytosis, thus reinforcing our results showing that the phagocytes from *P. lividus* take up PVP-AuNP aggregates/agglomerates very efficiently (Figure 2). Concordantly, guanosine monophosphate in the cyclic dimeric form (cGDP) activates and controls the innate immune response of mammalian dendritic cells, macrophages, and monocytes[57]. Notably, an increase in GMP as well as in UMP influence the immunological state of cells by increasing DNA replication, gene transcription and corresponding protein synthesis[58]. N-Acetylneuraminic acid (sialic acid) is widely expressed on the surfaces of all cells in all animals of the deuterostome lineage[59]. It is the major component of glycoconjugates as glycolipids, glycoproteins and proteoglycans. Reduced sialic acid expression induces maturation of mammalian dendritic cells that is correlated with tolerance induction through cytokine production[60]. Heparin sulfate liberated from the extracellular matrices by enzymes released during inflammation can promote immune activation by TLR4 signalling[61]. The trend of decreased amounts of sialic acid and sulfate metabolites in sea urchin cells exposed to PVP-AuNP (1 μg mL^{-1}) suggest an ongoing metabolic shift in these cells to a resolution of the inflammatory response. In general, these metabolic results highlight the broad metabolic plasticity of phagocytes in *P. lividus* and their related adaptations to nanoparticles.

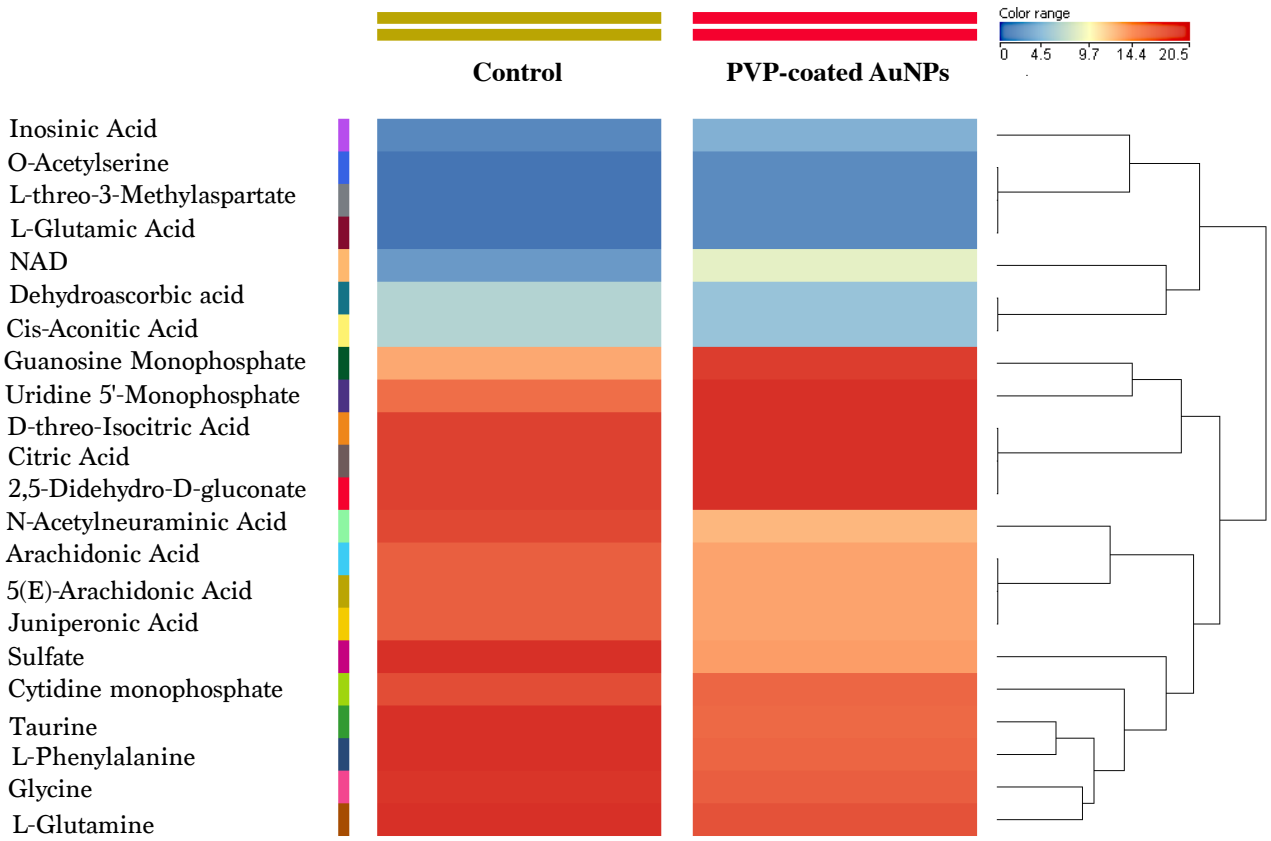

Figure 5. Sea urchin phagocytes show metabolic rewiring in response to PVP-AuNPs. Untargeted metabolic profiling of exposed (1 µg mL^{-1}, 24 h) and un-exposed phagocytes (control cells). Hierarchical clustering heatmaps display significantly ($p \leq 0.05$) different intracellular metabolites by LC-MS. Metabolic typing was performed on primary cultures of phagocytes from five individual *P. lividus* donors.

3.4 PVP-AuNP induce an increase in the levels of a few proteins involved in defensive innate/inflammatory signalling at the highest concentration

The decision process for an immune system to respond to "non-self" in one of many possible directions is determined by many elements acting synergistically through a hierarchically organised set of molecular networks that are dependent on dynamic changes in cellular metabolism as implied above (Figure 5). To profile the state of the sea urchin immune system, as implied from phagocyte exposure to PVP-AuNPs *in vitro*, we focused on the putative intracellular signalling that regulates the effector molecules that elicit specific immunological functions. Specifically, changes in the levels of a few proteins involved in canonical defensive innate/inflammatory signalling were evaluated. These included phagocyte levels of Toll-like receptor 4, 38 mitogen-activated protein kinase (p38 MAPK), p42/44 MAP Kinase (ERK), nuclear factor-κB (NF-κB), interleukin-6 (IL-6), heat shock protein 70 (HSP70), Manganese superoxide dismutase (MnSOD), and *P. lividus* cellular adhesion proteins (*Pl*-toposome, *Pl*-nectin), and a lectin (*Pl*-galectin-8), upon exposure to PVP-AuNPs (1 and 10 µg mL^{-1}) for 24 h *in vitro*. The biochemical analysis of sea urchin phagocytes exposed to PVP-AuNPs (1 µg mL^{-1}) was consistent with our previous observations (Figure 3) of the healthy state of these cells; the protein levels in exposed cells were not different from the controls (see Figure 6A,

6B). This was in agreement with our finding that changes in the metabolism of phagocytes from *P. lividus* regulates the metabolic plasticity and adaptation to PVP-AuNPs. The soluble substances from the phagocytes, including cytokines, metabolites, and adhesion proteins function to detect and respond to environmental changes, and if necessary, lead to inflammatory reactions. A successful immunological defensive immune response acts decisively to control and dominate an insult, but uncontrolled or excessive inflammation is detrimental.

Our findings emphasised that when sea urchin phagocytes were exposed to PVP-AuNPs at the highest concentration (10 μg $mL^{-1)}$, they activated an immunological response involving TLR4/ERK signalling pathway based on increased protein levels (see Figure 6A, 6B). This result was in agreement with a previous report that AuNPs induce cell proliferation through the ERK signalling pathway in human primary osteoblasts[62]. In analogy, previous studies on sea urchin immune cells exposed to TiO_2NPs underlined the involvement of the TLR4/p38 MAPK signalling pathway in the sea urchin phagocyte immune response *in vivo*[16]. Specifically, cells exposed to PVP-AuNPs (10 μg mL^{-1}) showed a 3-fold increase in TLR4 protein levels compared to the controls. Immunofluorescent images displayed that TLR4 was located on exposed-cells surfaces organized in clusters (Figure 6C, red spots). TLR4 is recruited to specific cell surface domains (lipid raft domains) to form nanoscale clusters when activated by a ligand[63]. In agreement, our result further supports the key role for TLR4 in PVP-AuNP-induced sea urchin inflammatory response. Furthermore, exposed cells showed a weak increase in the ERK phosphorylation level (1.5 fold), as well as a modest increase in the NF-κB and in the IL-6 intracellular level (2-fold increase each; Figure 6B). On the contrary, p38 MAPK phosphorylation (P-p38 MAPK) was not affected. NF-κB, the most sensitive transcription factor associated with responses related to inflammation, is known to be the final protein that functions in the TLR4/NF-κB signalling pathway. It controls the expression of an array of inflammatory cytokines[64] of which the IL-6 is a pleiotropic cytokine classified as pro-inflammatory, as well as the expression of adhesion proteins and antioxidant enzymes[65-66]. Phagocyte exposure to PVP-AuNPs (10 μg mL^{-1}) stimulated an increase of the mitochondrial antioxidant enzyme MnSOD (1.8-fold increase), whereas the NPs did not inhibit or enhance the level of HSP70 (Figure 6B). This finding highlighted that exposed cells amplified their antioxidant activity perhaps for protection from the harmful effects of ROS overproduction[67], but the cells did not activate an HSP70-dependent stress response, likely because particles did not induce unfolding and aggregation of cell proteins. Finally, immune cell adhesion proteins function in regulating several aspects of an immune response, including immune cell trafficking and activation of effector cells[68]. Two of the key cell adhesion proteins involved in sea urchins (*Pl*-nectin and *Pl*-galectin-8) were found significantly increased (3.5 and 2-fold increase respectively) in response to PVP-AuNPs. In mammals, galectin-8 activates dendritic cells and promotes cell cytoskeletal organisation, attachment, and spreading[69-70], while nectin is bound by immune receptors to mediate immune recognition[71].

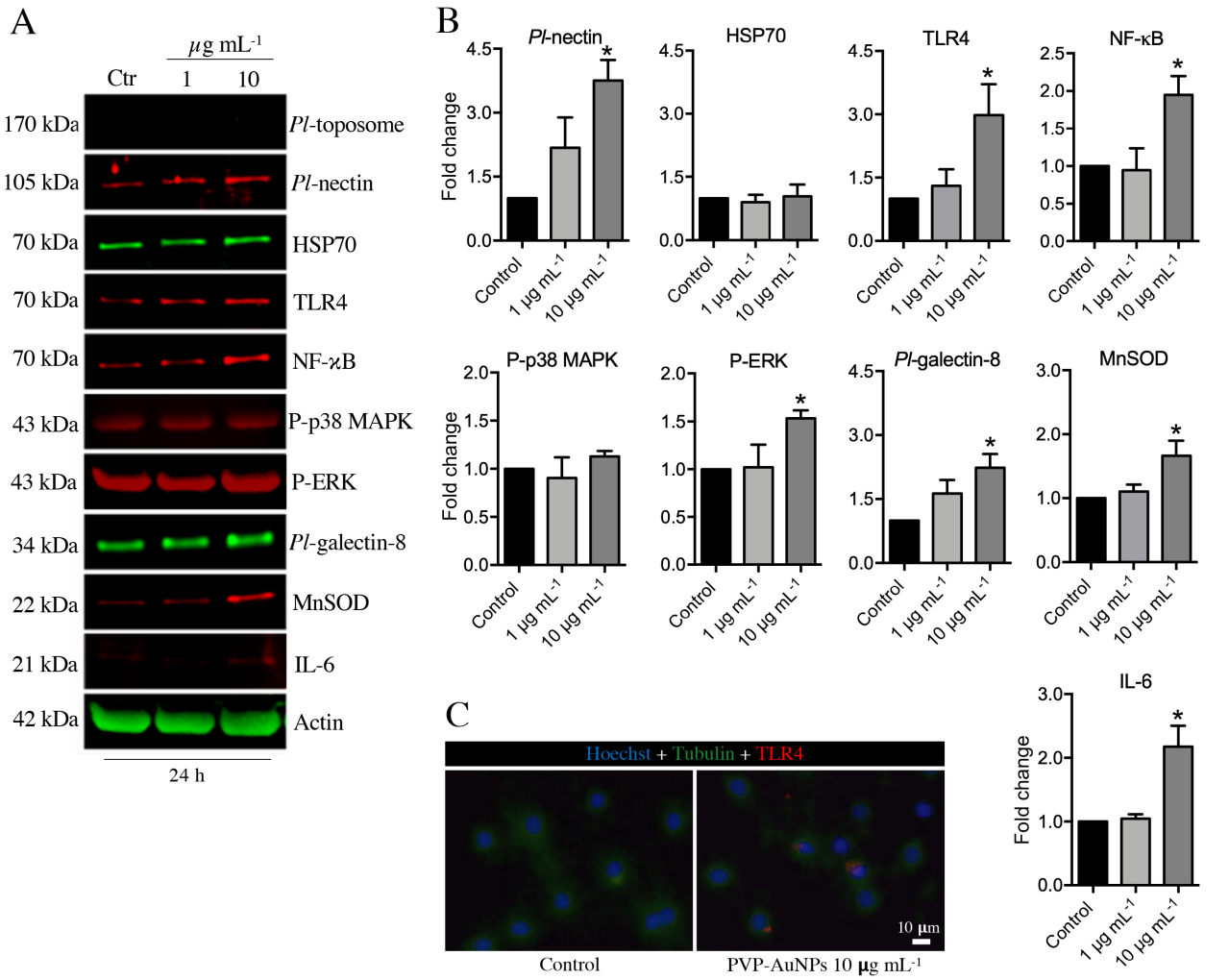

Figure 6. PVP-AuNP activate an immunological response involving TLR4/ERK signalling pathway at the highest concentration. (A) Representative immunoblotting shows results for the selected set of proteins in cells exposed to PVP-AuNPs (1 and 10 μg mL^{-1}) for 24 h. (B) Histograms representing the means ±SE of five replicates after normalisation with actin. Protein levels are expressed in arbitrary units as fold increase or decrease compared to controls that are set to 1. (C) Fluorescent imaging of phagocytes exposed to PVP-AuNPs (10 μg mL^{-1}) and control cells after 24 h. Cells are evaluated with TLR4 and tubulin antibodies. Immune cell nuclei are labelled with Hoechst 33342 (blue colour). Scale bar is 10 μm.

Overall, results show an astounding level of immunological plasticity, particularly at the higher concentration of particles (Figure 6), in which an efficient ongoing inflammatory state may progress a recovery-phase after three days of exposure (Figure 3). A summary view of the innate immune signalling in the interaction between sea urchin phagocytes and PVP–AuNPs is schematized in Figure 7, which underlines the putative role of each proteins found modulated at 10 μg mL^{-1} and 24 h of exposure. We speculate that the TLR4s activated by the PVP-AuNP-protein complexes, are recruited to specific cell surface domains promoting phagocytosis and related immune signalling cascade. Critically, we note that the complete categorized list of immune related genes in the sea urchin genome sequence include gene sequences that encode all of the proteins analysed here, excepting for IL-6. Failure to identify the IL-6 in the genome was because it was categorized with a set of genes for which no evident homology with human genes or with encoded proteins of similar

domain structure identified based on the search criteria detailed in the material and methods from Hibino et al[19]. Two explanations for this outcome may be i) there is a real absence of homologous genes encoding cytokines and chemokines in the echinoid lineage, or more likely ii) that the difficulties of detecting those genes is because they are small and evolve rapidly. Immunoblotting with IL-6 antibody shows a single immuno-reactive band of expected molecular weight only in stimulated cells, indicating that the antibody against human IL-6 is likely to cross-react with sea urchin IL-6. However, other plausible explanations cannot yet be excluded.

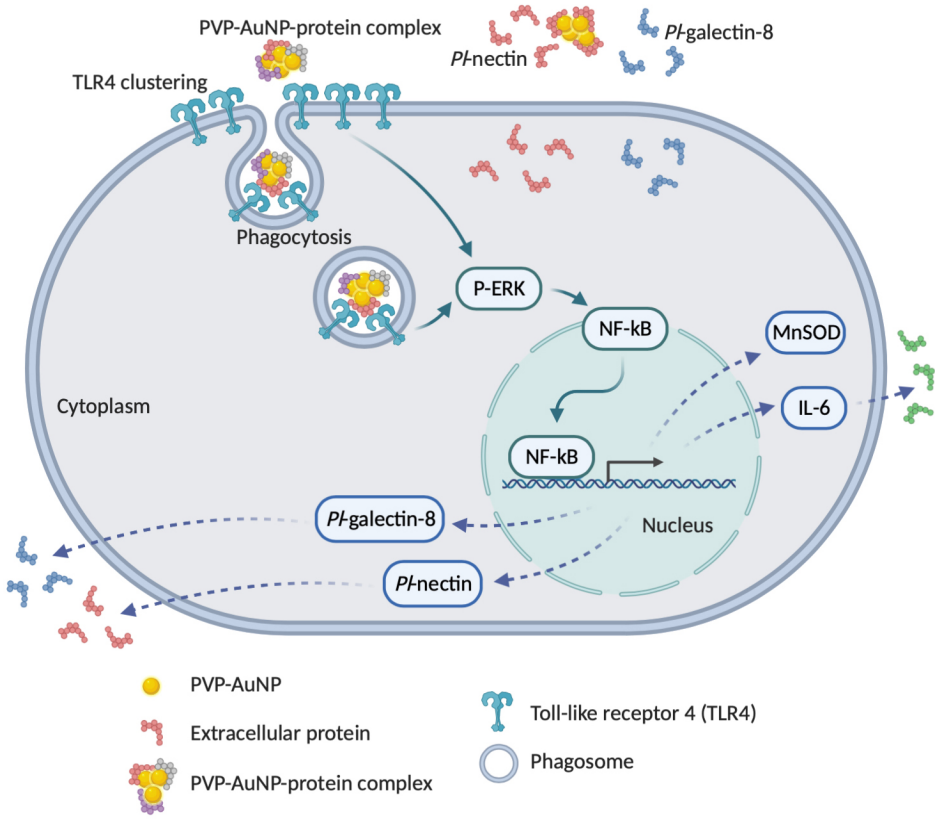

Figure 7. Schematic representation of the sea urchin immune signalling putatively involved in the response to PVP-AuNPs at the higher concentration of particles. Upon interaction with the CF, sea urchin extracellular proteins form a complex protein corona on PVP-AuNP surfaces. The TLR4s are recruited to specific cell surface domains to form dense nanoscale clusters because activated by a PVP-AuNP-protein complex (see TLR4 clustering), and promote phagocytosis and related immune signalling cascade. TLR4s initiate downstream signalling pathway by phosphorylation/activation of the p42/44 MAP Kinase (ERK) that leads to the NF-κB activation. The TLR4/NF-κB signalling activation induces the production of the antioxidant enzyme MnSOD, the cytokine IL-6, and the adhesion proteins *Pl*-nectin and *Pl*-galectin-8. The cell i) amplifies their antioxidant activity for protection from the harmful effects of ROS overproduction induced by the particle, ii) releases the *Pl*-galectin-8 for promote cell cytoskeletal re-organisation, attachment, and spreading, and iii) releases the *Pl*-nectin to take part in corona modelling mediating particle immune recognition. Created with BioRender.com.

4. CONCLUSIONS

Since the recognition by Metchnikoff of the biological role of echinoderm phagocytic cells in immunity[72] phagocytosis has been understood to function in all animals and is considered a key cellular mechanism in the resolution of inflammation and in activating signals that suppress the release of proinflammatory cytokines[73]. By studying the interactions between sea urchin phagocytes and PVP–AuNP *in vitro* we learned about the conserved mechanism of immune defence elicited by the gold particles at the nanoscale level of immune-machinery. The relationship between PVP-AuNP and the sea urchin phagocytes is established by the binding of a few extracellular proteins existing in the CF to the particle surface. Protein-particle interactions trigger an extended network of immune-related signalling in the phagocytes resulting in a transient immune activation both at the lower and higher concentration of the particles.

Functionalised particle surface with the PVP capping agent shows considerable particle stability in pure water and in CCM, confirming a strong steric stabilisation nature of this particle. The unexpected finding was that PVP does not favour hetero-aggregation in sea urchin CF in CCM, which differ from the CCM only in the presence of the biomacromolecules only. Sea urchin extracellular proteins promote a strong particle surface binding affinity but at the same time stimulate aggregation/agglomeration after 24 h of exposure. However, while customised AuNPs do not show expected stability during the exposure phase, our findings highlight the capability of particles to be transiently immunogenic at both these concentrations. Thus, PVP–AuNPs may be considered immunologically safe in organisms because they do not impair the physiological health of sea urchins, preserving the defensive responses, and do not cause a pathologically chronic inflammatory response with associated irreversible damage. Our results suggest that nano-immune studies in non-mammalian models that are *proxy for humans*, should be implemented and designed going over of apparent problems to successfully translate results to human immunity[74].

AUTHOR INFORMATION

Author Contributions

Andi Alijagic: investigation, validation, formal analysis **Francesco Barbero**: validation, formal analysis **Daniela Gaglio**: conceptualisation, methodology **Elisabetta Napodano**: conceptualisation, methodology. **Oldřich Benada**: investigation **Olga Kofroňová**: investigation. **Victor F. Puntes**: methodology, funding acquisition **Neus G. Bastús**: methodology **Annalisa Pinsino**: conceptualisation, data curation, supervision, writing-original draft, funding acquisition, project administration.

Funding Sources

This project has received funding from the European Union's Horizon 2020 research and innovation program under the Marie Skłodowska-Curie grant agreement [No 671881].

Notes

The authors declare no competing financial interest.

ACKNOWLEDGMENTS

The authors gratefully acknowledge Mr. M. Biondo for his technical support and sea urchin husbandry; Prof. L. Courtney Smith for English editing; Dr. R. Bonaventura, Dr. C. Costa, Dr. K. Karakostis, Dr. F. Zito for *Pl* antibodies; and the Electron Microscopy Facility of CAS (Prague, Czechia; supported by the project LO1509 of the Ministry of Education, Youth and Sports) for the electron microscopy images.

REFERENCES

1. Zhang, J., Mou, L., & Jiang, X. (2020). Surface chemistry of gold nanoparticles for health-related applications. *Chemical Science*.

2. Farooq, M. U., Novosad, V., Rozhkova, E. A., Wali, H., Ali, A., Fateh, A. A., Neogi, P. B., Neogi, A., & Wang, Z. (2018). Gold nanoparticles-enabled efficient dual delivery of anticancer therapeutics to HeLa cells. *Scientific reports*, 8(1), 1-12.

3. Nowack, B., Ranville, J. F., Diamond, S., Gallego-Urrea, J. A., Metcalfe, C., Rose, J., Horne, N., Koelmans, A. A., & Klaine, S. J. (2012). Potential scenarios for nanomaterial release and subsequent alteration in the environment. *Environmental toxicology and Chemistry*, *31*(1), 50-59.

4. López-Lorente, Á. I., & Valcárcel, M. (2014). Determination of Gold Nanoparticles in Biological, Environmental, and Agrifood Samples. In *Comprehensive Analytical Chemistry* (Vol. 66, pp. 395-426). Elsevier.

5. Boraschi, D., Italiani, P., Palomba, R., Decuzzi, P., Duschl, A., Fadeel, B., & Moghimi, S. M. (2017, December). Nanoparticles and innate immunity: new perspectives on host defence. In *Seminars in immunology* (Vol. 34, pp. 33-51). Academic Press.

6. Dykman, L. A., & Khlebtsov, N. G. (2017). Immunological properties of gold nanoparticles. *Chemical science*, 8(3), 1719-1735.

7. Shukla, R., Bansal, V., Chaudhary, M., Basu, A., Bhonde, R. R., & Sastry, M. (2005). Biocompatibility of gold nanoparticles and their endocytotic fate inside the cellular compartment: a microscopic overview. *Langmuir,* 21(23), 10644-10654.

8. Yen, H. J., Hsu, S. H., & Tsai, C. L. (2009). Cytotoxicity and immunological response of gold and silver nanoparticles of different sizes. *Small*, 5(13), 1553-1561.

9. Sumbayev, V. V., Yasinska, I. M., Garcia, C. P., Gilliland, D., Lall, G. S., Gibbs, B. F., Bonsall, D. R., Varani, L., Rossi, F., & Calzolai, L. (2013). Gold nanoparticles downregulate interleukin-1β-induced pro-inflammatory responses. *Small,* 9(3), 472-477.

10. le Guével, X., Palomares, F., Torres, M. J., Blanca, M., Fernandez, T. D., & Mayorga, C. (2015). Nanoparticle size influences the proliferative responses of lymphocyte subpopulations. *RSC Advances*, 5(104), 85305-85309.

11. Mahl, D., Greulich, C., Meyer-Zaika, W., Köller, M., & Epple, M. (2010). Gold nanoparticles: dispersibility in biological media and cell-biological effect. *Journal of Materials Chemistry*, 20(29), 6176-6181.

12. Tran, T. H., & Amiji, M. M. (2015). Targeted delivery systems for biological therapies of inflammatory diseases. *Expert opinion on drug delivery*, 12(3), 393-414.

13. Riediker, M., Zink, D., Kreyling, W., Oberdörster, G., Elder, A., Graham, U., Lynch, I., Duschl, A., Ichihara, G., Ichihara, S., & Kobayashi, T. (2019). Particle toxicology and health-where are we?. *Particle and fibre toxicology*, 16(1), 19.

14. Herrmann, K., Pistollato, F., & Stephens, M. L. (2019). Beyond the 3Rs: Expanding the use of human-relevant replacement methods in biomedical research. *ALTEX* 36(3), 343-352.

15. Falugi, C., Aluigi, M. G., Chiantore, M. C., Privitera, D., Ramoino, P., Gatti, M. A., Fabrizi, A., Pinsino, A., & Matranga, V. (2012). Toxicity of metal oxide nanoparticles in immune cells of the sea urchin. *Marine environmental research*, 76, 114-121.

16. Pinsino, A., Russo, R., Bonaventura, R., Brunelli, A., Marcomini, A., & Matranga, V. (2015). Titanium dioxide nanoparticles stimulate sea urchin immune cell phagocytic activity involving TLR/p38 MAPK-mediated signalling pathway. *Scientific reports*, 5, 14492.

17. Alijagic, A., Benada, O., Kofroňová, O., Cigna, D., & Pinsino, A. (2019). Sea urchin extracellular proteins design a complex protein corona on titanium dioxide nanoparticle surface influencing immune cell behaviour. *Frontiers in Immunology*, 10, 2261.

18. Alijagic, A., Gaglio, D., Napodano, E., Russo, R., Costa, C., Benada, O., Kofroňová, O., & Pinsino, A. (2020). Titanium dioxide nanoparticles temporarily influence the sea urchin immunological state suppressing inflammatory-relate gene transcription and boosting antioxidant metabolic activity. *Journal of hazardous materials*, 384, 121389.

19. Hibino, T., Loza-Coll, M., Messier, C., Majeske, A. J., Cohen, A. H., Terwilliger, D. P., Buckley, K. M., Brockton, V., Nair, S. V., Berney, K., & Fugmann, S. D. (2006). The immune gene repertoire encoded in the purple sea urchin genome. *Developmental biology*, 300(1), 349-365.

20. Bastús, N. G., Comenge, J., & Puntes, V. (2011). Kinetically controlled seeded growth synthesis of citrate-stabilized gold nanoparticles of up to 200 nm: size focusing versus Ostwald ripening. *Langmuir*, *27*(17), 11098-11105.

21. Henson, J. H., Svitkina, T. M., Burns, A. R., Hughes, H. E., MacPartland, K. J., Nazarian, R., & Borisy, G. G. (1999). Two components of actin-based retrograde flow in sea urchin coelomocytes. *Molecular biology of the cell*, 10(12), 4075-4090.

22. Pinsino, A., & Alijagic, A. (2019). Sea urchin *Paracentrotus lividus* immune cells in culture: formulation of the appropriate harvesting and culture media and maintenance conditions. *Biology open*, *8*(3), bio039289.

23. Pamies, R., Cifre, J. G. H., Espín, V. F., Collado-González, M., Baños, F. G. D., & de la Torre, J. G. (2014). Aggregation behaviour of gold nanoparticles in saline aqueous media. *Journal of nanoparticle research*, 16(4), 2376.

24. Barreto, Â., Luis, L. G., Girão, A. V., Trindade, T., Soares, A. M., & Oliveira, M. (2015). Behavior of colloidal gold nanoparticles in different ionic strength media. *Journal of Nanoparticle Research*, 17(12), 493.

25. Tomaszewska, E., Soliwoda, K., Kadziola, K., Tkacz-Szczesna, B., Celichowski, G., Cichomski, M., Szmaja, W., & Grobelny, J. (2013). Detection limits of DLS and UV-Vis spectroscopy in characterization of polydisperse nanoparticles colloids. *Journal of Nanomaterials*, 2013.

26. Ritchie, N. W. (2011). Getting Started with NIST* DTSA-II. *Microscopy Today*, *19*(1), 26-31.

27. Newbury, D. E., & Ritchie, N. W. (2013). Is scanning electron microscopy/energy dispersive X-ray spectrometry (SEM/EDS) quantitative?. *Scanning*, *35*(3), 141-168.

28. Pinsino, A., Roccheri, M. C., & Matranga, V. (2014). Manganese overload affects p38 MAPK phosphorylation and metalloproteinase activity during sea urchin embryonic development. *Marine environmental research*, *93*, 64-69.

747 29. Pinsino, A., Thorndyke, M., & Matranga, V. (2007). Coelomocytes and post-traumatic response in the
748 common sea star Asterias rubens. *Cell Stress & Chaperones*, *12*, 331-341.

749 30. Zito, F., Nakano, E., Sciarrino, S., & Matranga, V. (2000). Regulative specification of ectoderm in skeleton
750 disrupted sea urchin embryos treated with monoclonal antibody to Pl-nectin. *Development, growth &*
751 *differentiation*, *42*(5), 499-506.

752 31. Karakostis, K., Costa, C., Zito, F., & Matranga, V. (2015). Heterologous expression of newly identified
753 galectin-8 from sea urchin embryos produces recombinant protein with lactose binding specificity and anti-
754 adhesive activity. *Scientific reports*, *5*, 17665.

755 32. Jeevanandam, J., Barhoum, A., Chan, Y. S., Dufresne, A., & Danquah, M. K. (2018). Review on
756 nanoparticles and nanostructured materials: history, sources, toxicity and regulations. *Beilstein journal of*
757 *nanotechnology*, 9(1), 1050-1074.

758 33. Slomberg, D. L., Ollivier, P., Miche, H., Angeletti, B., Bruchet, A., Philibert, M., Brant, J., & Labille, J.
759 (2019). Nanoparticle stability in lake water shaped by natural organic matter properties and presence of
760 particulate matter. *Science of The Total Environment*, 656, 338-346.

761 34. Cohen, Y., Rallo, R., Liu, R., & Liu, H. H. (2013). In silico analysis of nanomaterials hazard and risk.
762 *Accounts of chemical research*, 46(3), 802-812.

763 35. Cosgrove, T. (Ed.). (2010). *Colloid science: principles, methods and applications*. John Wiley & Sons.

764 36. Koczkur, K. M., Mourdikoudis, S., Polavarapu, L., & Skrabalak, S. E. (2015). Polyvinylpyrrolidone (PVP)
765 in nanoparticle synthesis. *Dalton Transactions*, *44*(41), 17883-17905.

766 37. Tejamaya, M., Römer, I., Merrifield, R. C., & Lead, J. R. (2012). Stability of citrate, PVP, and PEG coated
767 silver nanoparticles in ecotoxicology media. *Environmental science & technology*, 46(13), 7011-7017.

768 38. Guerrini, L., Alvarez-Puebla, R. A., & Pazos-Perez, N. (2018). Surface modifications of nanoparticles for
769 stability in biological fluids. *Materials*, *11*(7), 1154.

770 39. Labille, J., Harns, C., Bottero, J. Y., & Brant, J. (2015). Heteroaggregation of titanium dioxide
771 nanoparticles with natural clay colloids. *Environmental science & technology*, *49*(11), 6608-6616.

772 40. Rostek, A., Mahl, D., & Epple, M. (2011). Chemical composition of surface-functionalized gold
773 nanoparticles. *Journal of Nanoparticle Research*, 13(10), 4809-4814.

774 41. Barbero, F., Moriones, O. H., Bastús, N. G., & Puntes, V. (2019). Dynamic Equilibrium in the
775 Cetyltrimethylammonium Bromide–Au Nanoparticle Bilayer, and the Consequent Impact on the Formation of
776 the Nanoparticle Protein Corona. *Bioconjugate Chemistry*, *30*(11), 2917-2930.

777 42. Su, K. H., Wei, Q. H., Zhang, X., Mock, J. J., Smith, D. R., & Schultz, S. (2003). Interparticle coupling
778 effects on plasmon resonances of nanogold particles. *Nano letters*, *3*(8), 1087-1090.

779 43. Park, J., Park, J. H., Ock, K. S., Ganbold, E. O., Song, N. W., Cho, K., Lee, S. Y., & Joo, S. W. (2011).
780 Preferential adsorption of fetal bovine serum on bare and aromatic thiol-functionalized gold surfaces in cell
781 culture media. *Journal of colloid and interface science*, *363*(1), 105-113.

782 44. Podila, R., Chen, R., Ke, P. C., Brown, J. M., & Rao, A. M. (2012). Effects of surface functional groups
783 on the formation of nanoparticle-protein corona. *Applied physics letters*, 101(26), 263701.

784 45. Lu, X., Xu, P., Ding, H. M., Yu, Y. S., Huo, D., & Ma, Y. Q. (2019). Tailoring the component of protein
785 corona via simple chemistry. *Nature communications*, 10(1), 1-14.

786 46. Pinsino, A., & Matranga, V. (2015). Sea urchin immune cells as sentinels of environmental
787 stress. *Developmental & Comparative Immunology*, *49*(1), 198-205.

47. Smith, L. C., Arizza, V., Hudgell, M. A. B., Barone, G., Bodnar, A. G., Buckley, K. M., Cunsolo, V., Dheilly, N. M., Franchi, N., Fugmann, S. D., Furukawa, R., Garcia-Arraras, J., Henson, J. H., Hibino, T., Irons, Z. H., Li, C., Man Lun, C., Majeske, A. J., Oren, M., Pagliara, P., Pinsino, A., Raftos, D. A., Rast, J. P., Samasa, B., Schillaci, D., Schrankel, C. S., Stabili, L., Stensväg, K., & Sutton, E. (2018). Echinodermata: the complex immune system in echinoderms. In: Cooper, E.L. (Ed.), *Advances in Comparative Immunology*. Springer International Publishing AG, pp. 409–501.

48. Goldstein, A., Soroka, Y., Frušić-Zlotkin, M., Popov, I., & Kohen, R. (2014). High resolution SEM imaging of gold nanoparticles in cells and tissues. *Journal of microscopy*, *256*(3), 237-247.

49. Mironava, T., Hadjiargyrou, M., Simon, M., Jurukovski, V., & Rafailovich, M. H. (2010). Gold nanoparticles cellular toxicity and recovery: effect of size, concentration and exposure time. *Nanotoxicology*, *4*(1), 120-137.

50. Melillo, D., Marino, R., Italiani, P., & Boraschi, D. (2018). Innate immune memory in invertebrate metazoans: a critical appraisal. *Frontiers in immunology*, 9, 1915.

51. Ding, L., Yao, C., Yin, X., Li, C., Huang, Y., Wu, M., Wang, B., Guo, X., Wang, Y., & Wu, M. (2018). Size, shape, and protein corona determine cellular uptake and removal mechanisms of gold nanoparticles. *Small*, *14*(42), 1801451.

52. Chen, F., Wang, G., Griffin, J. I., Brenneman, B., Banda, N. K., Holers, V. M., Backos, D. S., Wu, L., Moghimi, S. M., & Simberg, D. (2017). Complement proteins bind to nanoparticle protein corona and undergo dynamic exchange in vivo. *Nature nanotechnology*, *12*(4), 387.

53. Zhang, S., Bories, G., Lantz, C., Emmons, R., Becker, A., Liu, E., Abecassis, M. M., Yvan-Charvet, L., & Thorp, E. B. (2019). Immunometabolism of phagocytes and relationships to cardiac repair. *Frontiers in cardiovascular medicine*, *6*.

54. Liaudet, L., Mabley, J. G., Pacher, P., Virág, L., Soriano, F. G., Marton, A., Haskó, G., Deitch, E. A., & Szabó, C. (2002). Inosine exerts a broad range of antiinflammatory effects in a murine model of acute lung injury. *Annals of surgery*, *235*(4), 568.

55. Minhas, P. S., Liu, L., Moon, P. K., Joshi, A. U., Dove, C., Mhatre, S., Contrepois, K., Wang, Q., Lee, B. A., Coronado, M., & Bernstein, D. (2019). Macrophage de novo NAD+ synthesis specifies immune function in aging and inflammation. *Nature immunology*, *20*(1), 50-63.

56. Venter, G., Oerlemans, F. T., Willemse, M., Wijers, M., Fransen, J. A., & Wieringa, B. (2014). NAMPT-mediated salvage synthesis of NAD+ controls morphofunctional changes of macrophages. *PLoS One*, *9*(5).

57. Cui, T., Cang, H., Yang, B., & He, Z. G. (2019). Cyclic dimeric guanosine monophosphate: activation and inhibition of innate immune response. *Journal of innate immunity*, *11*(3), 242-248.

58. Lane, A. N., & Fan, T. W. M. (2015). Regulation of mammalian nucleotide metabolism and biosynthesis. *Nucleic acids research*, *43*(4), 2466-2485.

59. Varki, A., & Gagneux, P. (2012). Multifarious roles of sialic acids in immunity. *Annals of the New York Academy of Sciences*, *1253*(1), 16.

60. Lübbers, J., Rodríguez, E., & Van Kooyk, Y. (2018). Modulation of immune tolerance via Siglec-sialic acid interactions. *Frontiers in Immunology*, *9*, 2807.

61. Collins, L. E., & Troeberg, L. (2019). Heparan sulfate as a regulator of inflammation and immunity. *Journal of leukocyte biology*, *105*(1), 81-92.

62. Zhang, D., Liu, D., Zhang, J., Fong, C., & Yang, M. (2014). Gold nanoparticles stimulate differentiation and mineralization of primary osteoblasts through the ERK/MAPK signaling pathway. *Materials Science and Engineering: C*, *42*, 70-77.

831 63. Płóciennikowska, A., Hromada-Judycka, A., Borzęcka, K., & Kwiatkowska, K. (2015). Co-operation of
832 TLR4 and raft proteins in LPS-induced pro-inflammatory signaling. *Cellular and molecular life sciences*,
833 72(3), 557-581.

834 64. Kawai, T., & Akira, S. (2007). Signaling to NF-κB by Toll-like receptors. *Trends in molecular*
835 *medicine*, *13*(11), 460-469.

836 65. Lockyer, J.M., Colladay, J.S., Alperin-Lea, W.L., Hammond, T., & Buda A.J. (1998). Inhibition of nuclear
837 factor-κb–mediated adhesion molecule expression in human endothelial cells *Circulation Research*, *82, 314–*
838 *320.*

839 66. Yuan, S., Liu, X., Zhu, X., Qu, Z., Gong, Z., Li, J., Xiao, L., Yang, Y., Liu, H., Sun, L., & Liu F. (2018).
840 The role of TLR4 on PGC-1α-mediated oxidative stress in tubular cell in diabetic kidney disease. *Oxidative*
841 *Medicine and Cellular Longevity,* 2018, 6296802.

842 67. Abdal Dayem, A., Hossain, M. K., Lee, S. B., Kim, K., Saha, S. K., Yang, G. M., Choi, H. Y., & Cho, S.
843 G. (2017). The role of reactive oxygen species (ROS) in the biological activities of metallic
844 nanoparticles. *International journal of molecular sciences*, *18*(1), 120.

845 68. Harjunpää, H., Llort Asens, M., Guenther, C., & Fagerholm, S. C. (2019). Cell adhesion molecules and
846 their roles and regulation in the immune and tumor microenvironment. *Frontiers in Immunology*, 10, 1078.

847 69. Levy, Y., Arbel-Goren, R., Hadari, Y. R., Eshhar, S., Ronen, D., Elhanany, E., Geiger, B., & Zick, Y.
848 (2001). Galectin-8 functions as a matricellular modulator of cell adhesion. *Journal of Biological*
849 *Chemistry*, *276*(33), 31285-31295.

850 70. Carabelli, J., Quattrocchi, V., D'Antuono, A., Zamorano, P., Tribulatti, M. V., & Campetella, O. (2017).
851 Galectin-8 activates dendritic cells and stimulates antigen-specific immune response elicitation. *Journal of*
852 *leukocyte biology*, *102*(5), 1237-1247.

853 71. Gao, G. (2013). Nectin and nectin-like molecules: immune regulator, adhesion molecule and virus
854 receptors (P1001).

855 72. Gordon, S. (2016). Phagocytosis: the legacy of Metchnikoff. *Cell*, 166(5), 1065-1068.

856 73. Maderna, P., & Godson, C. (2003). Phagocytosis of apoptotic cells and the resolution of inflammation.
857 *Biochimica et Biophysica Acta (BBA) - Molecular Basis of Disease, 1639*(3), 141-151.

858 74. Boraschi, D., Alijagic, A., Auguste, M., Barbero, F., Ferrari, E., Hernadi, S., Mayall, M., Michelini, S.,
859 Navarro Pacheco, N. I., Prinelli, A., Swart, E., Swartzwelter, B. J., Bastús, N. G., Canesi, L., Drobne, D.,
860 Duschl, A., Ewart, M., Horejs-Hoeck, J., Italiani, P., Kemmerling, B., Kille, P., Prochazkova, P., Puntes, V.
861 F., Spurgeon, D. J., Svendsen, C., Wilde, C. J., & Pinsino, A. (2020). Addressing Nanomaterial Immunosafety
862 by Evaluating Innate Immunity across Living Species. *Small*, 2020, 2000598.